Proceedings of the 1st Global Power and Propulsion Forum
GPPF 2017
Jan 16-18, 2014, Zurich, Switzerland
www.pps.global

GPPF-2017-58

UNSTEADY VORTEX INTERACTION NEAR TURBINE ROTOR TIP AND ITS LOSS MECHANISM

Kai ZHOU
College of Engineering, Peking University
kinozhou@pku.edu.cn
Beijing, 100871, China

Chao ZHOU
College of Engineering, Peking University
czhou@pku.edu.cn
Beijing, 100871, China

ABSTRACT

In an unshrouded high-pressure turbine, tip leakage flow causes a loss of efficiency. The loss mechanisms of tip leakage flow were investigated mostly with steady incoming flows in previous studies. This paper will investigate the aerodynamic performance of the tip leakage flow in a turbine stage by solving Unsteady Reynolds-Averaged Navier-Stokes (URANS) equations. The unsteady results are also compared with results obtained by the steady simulation. Cases without rotor tip clearances are also simulated to understand the entropy generation due to the tip leakage flows.

The unsteady effects of the incoming vortex on the tip aerodynamic performance is found to be different from its effects on the hub region, where loss was considered to increase with incoming vortex. The tip leakage loss reduces due to the unsteady interaction of the incoming casing vortex and the flow near the rotor tip. In the steady calculation, tip leakage vortex breakdown occurs. The unsteady results show that the stator casing vortex tends to increase the minimum pressure at the center of the tip leakage loss core. As a result, the vortex interaction suppresses this vortex breakdown, thus reducing the loss. Without the tip clearance, vortex breakdown no longer occur near the tip with steady calculation. As a result, the unsteady effects of incoming vortex increases the loss. The time-averaged entropy generation of unsteady tip leakage vortex is 18% less than the loss in the steady case.

INTRODUCTION

In an unshrouded high pressure turbine, the pressure difference between the blade pressure side and the suction side drives the leakage flow across the tip gap between the rotor blade and the casing. The tip leakage flow is an important source of loss, which could account for as much as one-third of the losses in a turbine stage (Schaub et al. [1]). The pressure at the center of the tip leakage vortex is relatively low. Due to the adverse pressure gradient along the streamwise direction, the flow at the center of the vortex tends to reverse, which could lead to vortex breakdown. Vortex breakdown is considered as the detrimental loss of rotor tip leakage vortex (Huang et al. [2] and Gao et al. [3]).

Many studies aims to reduce the tip leakage loss. However, most understanding of the tip leakage flow is based on models with the steady inlet conditions, e.g. Key [4], Schabowski[5], Camciet et al.[6], Zhou et al. [7] and Zhang et al. [8]. In a turbine, the upstream blade row passes periodically relative to the downstream blade row, so the flow is inherently unsteady. The understanding of the effects of periodic unsteadiness on the flow field can result in an improvement of the turbine design (Denton [9]).

Quite a few studies investigates the effects of unsteadiness in the past two decades, e.g. Binder [10], Sharma et al. [11] and Dunn [12]. Based on the location, the effects of unsteadiness can be roughly classified as: 1. the region in the middle span blade surface where the blade-to-blade interaction and wake-blade interaction accounts; 2. the region near the blade hub where hub corner vortex plays an important role; 3. the region near the tip and casing where tip leakage flow dominates.

The effects of wake-blade interaction has been intensively investigated. Hodson [13] was among the first to utilize the upstream periodic wakes to control bypass transition and flow separations over the turbine blade. This mechanism can be used to increase the turbine loading with little aerodynamic penalty (Hodson and Howell [14]).

The vortex interaction near the hub region was studies in many works like Jenny et al. [15] and Schlienger et al. [16]. Pullan[17] suggested that the flow patterns depended on the specific design of the turbine, and the vortex interaction could be different for different turbines. The incoming vortex from the upstream stator interacts with the hub corner vortex in the rotor periodically, which was found to increase the loss of turbine. The unsteady loss is generated due to the extra shear stress in the rotor passage. Chaluvadi et al. [18][19] and Yoon[20]showed that unsteadiness simulation resulted in higher loss than that of the steady calculation.

The effects of the periodic unsteady interaction between the incoming stator passage vortex and the downstream rotor tip leakage vortex are less studied. Such interaction can cause complex flow physics, which is not well understood. Zeschky[21] mentioned that tip leakage vortex was only slightly affected by the passing stator wakes. Volino et al. [22] used Particle Image Velocimetry (PIV) to investigate the effects

of the upstream bar wake on the tip leakage flow in a cascade. They found that the effects of the unsteady wake were small. These studies actually investigated the wake-vortex interaction, which cannot represents the vortex-vortex interaction near the rotor tips. In Liu et al. [23], where the main focus is mainly on the unsteady effects on the tip heat transfer in a turbine stage, they found significant pressure variation at the 95% radial span of the blade. This shows that the vortex-vortex could result in noticeable effects on the flow physics of the tip leakage flow. However, it is still not clear the flow physics of the vortex-vortex interaction in the tip region of the rotor tip and its loss mechanism.

The current work aims to understand the effects of periodic unsteadiness on the aerodynamic performance of the tip leakage flow in a high-pressure turbine stage. The analysis focus on the flow physics due to the unsteady vortices interaction between the incoming stator casing vortex and the tip leakage vortex. Based on the flow physics, the loss mechanisms are discussed.

NUMERICAL METHODS

Geometry and Mesh

The subsonic high-pressure turbine stage used in this study is shown in Fig. 1. The entire computational domain consists of a stator domain and a rotor domain. The ratio of stator blade number and rotor blade number is 1:2. The rotor blade is twisted and has a flat tip geometry.

The boundary condition for the turbine stage is representative for engine operation. The total to static pressure ratio for the stage is 2.95 and the relative Mach number at the rotor exit is 0.83. The Reynolds number based on the axial chord is 1.5×10^6. The tip gap between the rotor tip and the casing is 1% of span. The reduced frequency *fr* based on the rotor axial chord is 0.48. In the steady calculation, the mixing plane model is used on the interface between stator domain and rotor domain. For unsteady calculation, sliding mesh is adopted at the interface. Two setups with 24 and 48 time steps are used for one stator-passing period time τ_0. The difference of time-averaged loss over one stator passing period between the two cases is less than 0.1%. The setup with 48 time steps will be used for analysis in this paper.

The computational mesh is generated by commercial software ICEM CFD with hexahedron grids. O-grid is used around the blade surface. The averaged y+ on the blade surface is 1.6 and the maximum y+ on the wall surface is less than 5. The growing ratio of the mesh is less than 1.3.

Mesh sensitivity is conducted with study RANS as shown in Fig. 2. The turbine stage efficiency changes less than 0.2% as the overall grid number changes from 7.2 million to 11.0 million. The overall mesh size of 10.3 million is used for the following analysis. The mesh on the cut plane of 0.5Cx in the rotor domain is shown in Fig. 3. Within the tip clearance, 34 grids are used. The mesh near the trailing edge is also shown in Fig. 3.

The case is considered converged when the change of root mean square of entropy rise for extra 2000 iterations over the cut plane of 1.5Cx is less than 0.1% the steady calculation. For the unsteady calculation, the difference of the time-averaged entropy over the same cut plane for two continuous stator-passing periods is less than 0.1% when the case is converged.

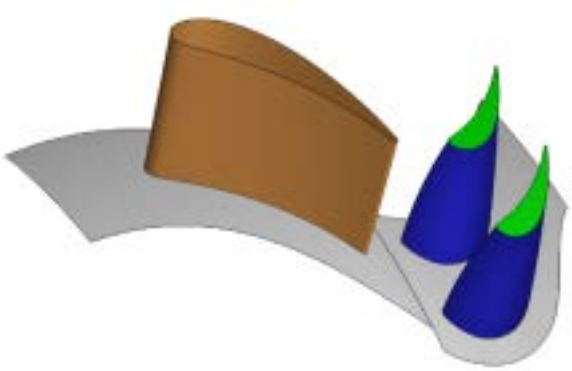

Fig. 1 Computational Domain with a Rotor Flat Tip

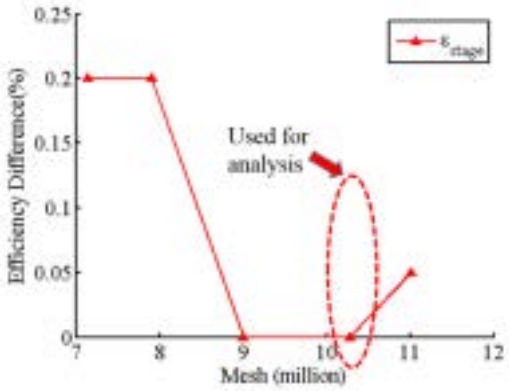

Fig. 2 Mesh Sensitivity Study

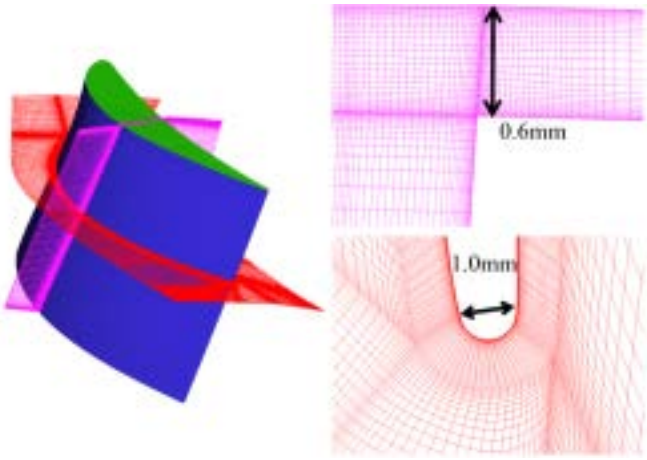

Fig. 3 Mesh on the Cut Planes of 0.5Cx and Near Trailing Edge

Turbulence Models and Validation

The commercial solver FLUENT is used to solve the steady and unsteady RANS equations. The turbulence model used in the current study is a two-equation shear stress transport model (Mentor [24], Smith [25]). 2nd order scheme with implicit solution method is used for discretizing the URANS equations.

Because there is no available unsteady experimental data of the current turbine, a transonic turbine cascade were simulated for the purpose of CFD validation. The experimental setup of Zhang et al. [26] is adopted. The exit Mach number equals 1.0 and the Reynolds number based on the axial chord is 1.27×10^6. The tip gap is 1.5% of the span. The isentropic Mach number is defined related to the static pressure.

Fig. 5 shows that the predicted static pressure along the blade well agrees with the experiment. Fig. 6 shows the heat

transfer coefficient on the tip surface shows similar effects of the flow physics within the tip gap.

The ability of CFD tool in prediction the unsteady flow physics is also validated based on the detailed unsteady measurement of T106C cascade, which can be found in Zhou [27]. The CFD tool can well simulate the unsteady flow physics, such as the transportation of the wakes and the development of turbulence kinetic energy.

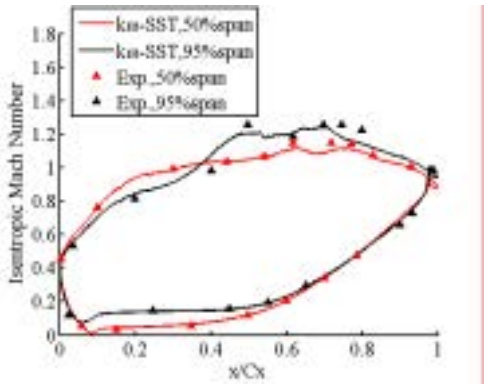

Fig. 4 Isentropic Mach Number Distribution along the Blade Middle Span and Near the Tip Region (Experimental Data from Zhang et al. [26])

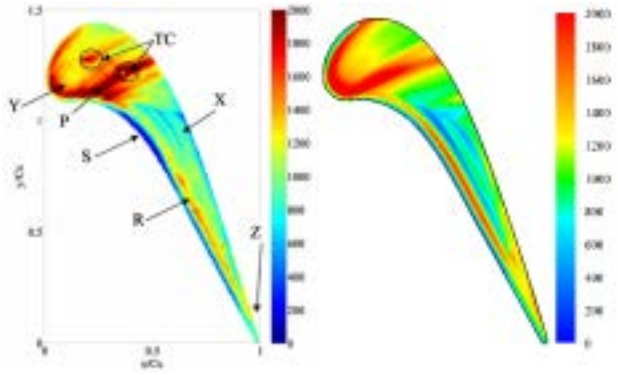

(a) Experiment (b) CFD

Fig. 5 Heat Transfer Coefficient (W/m^{2}K) on the Blade Tip by (a) Experiment (from Zhang et al.[26]) and (b) CFD

RESULTS AND DISCUSSION

Steady Results

The loss is expressed in terms of entropy, which is defined as:

$$\Delta s = s - s_{ref} = c_p \ln(\frac{T}{T_{in}}) - R \ln(\frac{p}{p_{in}}) \quad \text{Eq. 1}$$

Fig. 6 shows the entropy increase across the stage obtained with steady RANS method (SF) and Unsteady RANS method (UF). The magnitude of the entropy increase is normalized by the entropy increase when the flow exit the rotor of SF case is mixed-out. The red line represents the time-averaged unsteady entropy increase of UF along the axial chord. The variation of the local entropy is also indicated for the unsteady results. The entropy increase in the stator passage is similar for the steady and the unsteady simulation. For the unsteady simulation, a sudden increase of the entropy does not occur on the domain interface because the upstream flow passes smoothly across this interface. The time-averaged entropy generation in the unsteady calculation is lower than that in steady calculation across the rotor domain, which indicates that the unsteady interaction suppresses the loss developed in the rotor domain.

For the unsteady results, Fig. 6 shows that the variation of the entropy with time is small across the stator domain. In the gap between the stator and the rotor, the entropy varies due to the unsteady pressure distribution as the blade passes periodically. As suggested by Binder [10], the effects of the pressure field decays quickly downstream of rotor leading edge.

From the 0.3Cx to downstream, the unsteady loss variation is significant, mainly due to the transportation of the incoming vortices (including wakes) and its interaction within the rotor passage. The tip leakage flow and the endwall secondary flow have a large effect on the flow field. The following paper will focus on unsteady interaction of the flow near the rotor tip region.

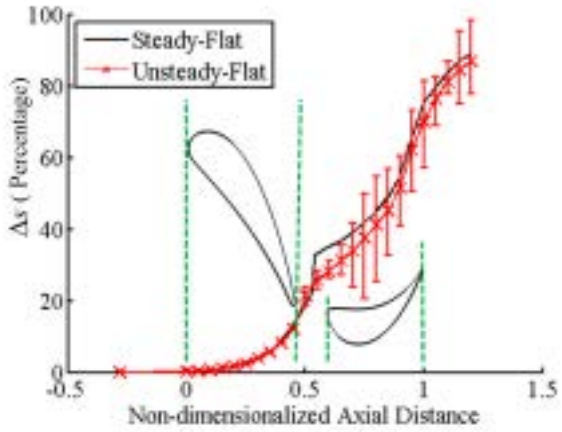

Fig. 6 Entropy Variation along Axial Direction for 'SF' and 'UF', Normalized by the Mixed Out Entropy in 'SF'

In the SF case, the limiting streamline on the rotor suction surface is shown in Fig. 7(a). The distribution of entropy are shown on four cut planes, which are perpendicular to the suction surface as SP60, SP65, SP75 and SP85. Only the area with entropy higher than 60 Jkg^{-1}K^{-1} is shown. The tip leakage flow cause an area of high entropy. The low kinetic energy flow in the boundary layer on the casing is driven by the pressure gradient in the blade passage and rolls up forming the secondary passage vortex. Due to the scraping effect of the casing motion, the shear stress also contributes the secondary flow. The separation line 'A' and reattachment line 'B' are shown in Fig. 7(a). When the main flow convects downstream, the tip leakage flow develops and entropy rises. In the center of vortex core, the pressure induced by the streamwise vortex reduces so that the flow suffers adverse pressure gradient, which decelerates flow. On planes of SP65, SP75 and SP85, negative velocity along the streamwise direction occurs as circled by the black lines. On SP65, the flow at the center of the tip leakage vortex starts to reverse, which causes vortex breakdown. The reversed flow region significantly enhances flow mixing, thus increasing loss. When the vortex convects downstream, the area of vortex breakdown increases because of the adverse pressure gradient as the main flow diffuses.

Fig. 7(b) shows the case of SNC, where the size of the tip gap is set as zero. For the SNC, only the secondary passage vortex loss can be identified near the tip, which is smaller than that in the SF case. This suggests that near the tip, the passage

vortex and the tip leakage vortex induce and enhance each other.

The streamwise vorticity overlaid by vortex breakdown region is shown in Fig. 8. The vorticity magnitude of the passage vortex in the SF case is much larger than that of the SNC. The strong positive vorticity at the center of the tip leakage vortex coincides with high entropy rise. However, at the SP75, the vorticity magnitude is lower than that at the SP65. This is because the large vortex structure breaks down into small scales to balance the adverse pressure gradient.

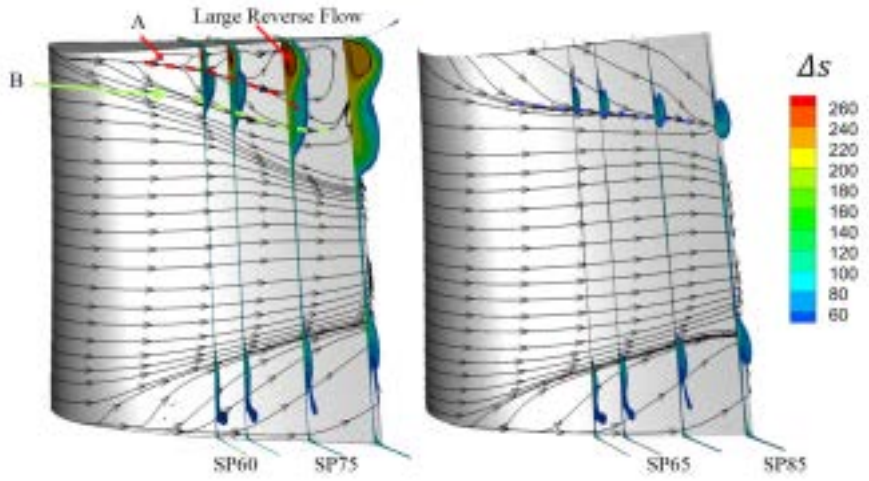

(a) SF case (b) SNC case

Fig. 7 Limiting Streamlines on Suction Surface and Entropy Rise ($Jkg^{-1}k^{-1}$) for 'SF' and 'SNC'

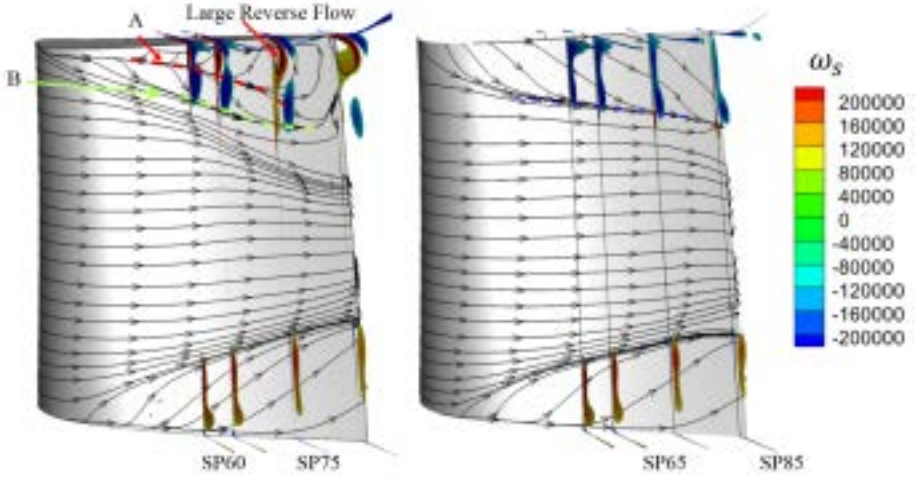

(a) SF case (b) SNC case

Fig. 8 Limiting Streamlines on Suction Surface and Streamwise Vorticity for 'SF' and 'SNC'

The leakage loss is defined as the difference of the integral entropy over the same cut plane between the SF and SNC cases. The entropy rate of tip leakage loss is then defined as the entropy generation per unit length along the axial direction, as shown in Fig. 9. It increases rapidly downstream of 0.7Cx where the vortex breakdown just occurs. The maximum of loss rate occurs at 0.88Cx plan where the largest turbulent shear stress occurs. Axial cut plane surfaces are divided at middle span to access the loss near the tip (Half Casing) and the hub (Half Hub). Near the rotor hub, Fig. 10(a) shows that both the SF case and SNC case have the similar loss rate distribution. In Fig. 10(b), the SF case has the larger entropy rate from 0.5Cx and the sharp peak loss rate near the trailing edge than that of the SNC. This large entropy rate is caused by the tip leakage vortex breakdown from 0.7Cx to trailing edge.

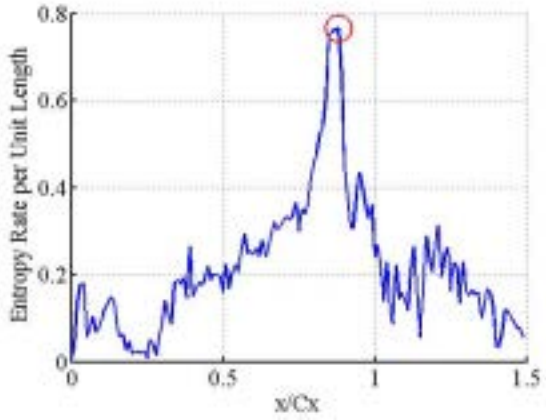

Fig. 9 Tip Leakage Loss per Unit Length (JK^{-1}) Along Axial Direction

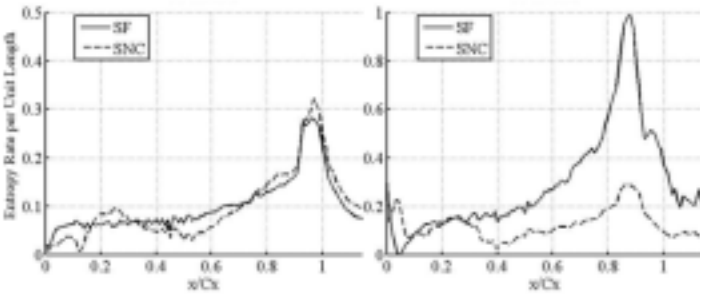

(a) Half Hub (b) Half Casing

Fig. 10 Entropy Rise Rate (JK^{-1}) for Two Passages

Unsteady Results

The analysis with steady simulation shows that the tip leakage vortex breakdown significantly increases the entropy generation. The following analysis based on the unsteady simulation will show and explain that the unsteady vortex interaction suppress the vortex breakdown, which is aerodynamically beneficial.

Fig. 11 shows entropy contour at six equal time spaced instants. The surfaces from the upstream to downstream are SP60, SP65, SP70, SP75, SP80 and SP85, which are perpendicular to the suction surface side. Only the entropy contour above 60 $Jkg^{-1}K^{-1}$ is shown. The dark lines circle the regions with negative streamwise velocity representing the reversed flow. The loss associated with the tip leakage flow varies significantly when the upstream stator passage vortex passes.

In the steady case SF, the vortex breakdown occurs at the SP65. But in the unsteady case UF, vortex breakdown was pushed downstream due to the unsteady vortex interaction. At t/τ_0=2/48, the upstream stator casing passage vortex starts to interacts with the tip leakage vortex at the plane SP60. This reduces the entropy generation in the tip leakage vortex at this plane. Meanwhile, at t/τ_0=2/48, the occurrence of vortex breakdown appears at the SP75.

At the next time instant of t/τ_0=10/48, the stator passage vortex convects downstream to SP70, and the entropy generation of the tip leakage vortex reduces. The vortex breakdown is pushed further downstream to the SP85. The effects of incoming vortex is similar at the next time instant of t/τ_0=18/48.

After t/τ_0=26/48, the vortex originates from the stator travels to a location downstream of SP85, and its effect on the suppression of the tip leakage vortex breakdown reduces. The tip leakage vortex grows stronger and the vortex breakdown occurs at the SP70. At and t/τ_0=34/48 and t/τ_0=42/48, the vortex breakdown phenomena is similar to that obtained based on the steady simulation.

In this entire period, the incoming vortex suppresses the tip leakage vortex breakdown for more than half of the period, which reduces the loss.

In order to explore the mechanism for the suppression of the vortex breakdown, the flow pattern on the cut plane of 95% span at two typical time instants are presented in Fig. 12 and Fig. 13. Fig. 12 shows the entropy distribution, which is used to identify the location of the upstream vortices. This cut plane cuts across the center of the tip leakage vortex at 0.8Cx. At t/τ_0=10/48, the first incoming vortices passes across the cut plane of 0.8Cx, as shown by '1'. At time t/τ_0=34/48, the first vortices convects downstream and the second vortices is still far away from the cut plane of 0.8Cx.

The static pressure coefficient distributions at the same time instances are shown in Fig. 13. At t/τ_0=10/48 (Fig. 13b), when the first upstream vortices is located near the cut plane of 0.8Cx, the pressure in the tip leakage vortex is higher than the situation at time t/τ_0=34/48 (Fig. 13b). In other word, the stator vortex reduces the streamwise adverse pressure gradient. So, the vortex breakdown due to the adverse pressure is suppressed.

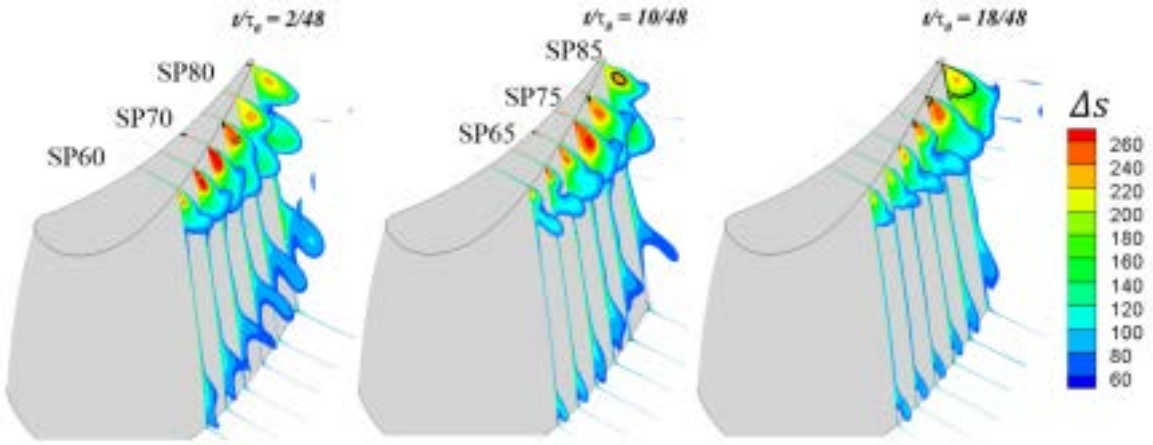

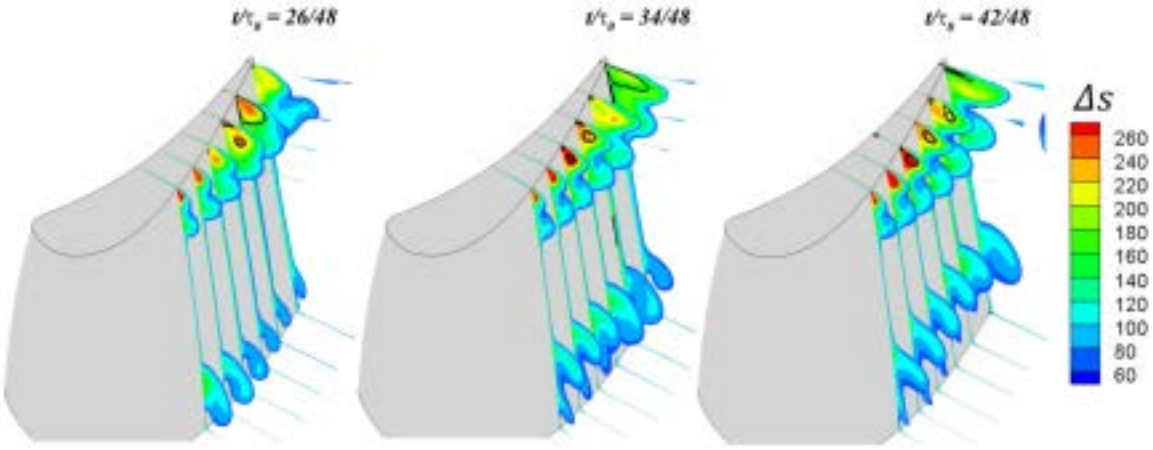

Fig. 11 Unsteady Resolutions of Entropy (Jkg^{-1}K^{-1}) in 'SF' on Six Planes: SP60, SP65, SP70, SP75, SP80 and SP85

Unsteady simulation was also run for the case without tip clearance. The entropy different between the case with tip clearance gap and without tip clearance gap is used to indicate the loss due to the tip leakage flow. Fig. 15 shows the normalized entropy generation due to tip leakage flow. With periodic incoming flow, the entropy generation at the exit of the rotor varies significantly. The maximum entropy generation with unsteady flows is slightly higher than that of the steady case. The minimum entropy generation with unsteady incoming flow is about half of that with steady flows. The loss of tip leakage flow reduced by 18% due to the unsteady vortex interaction.

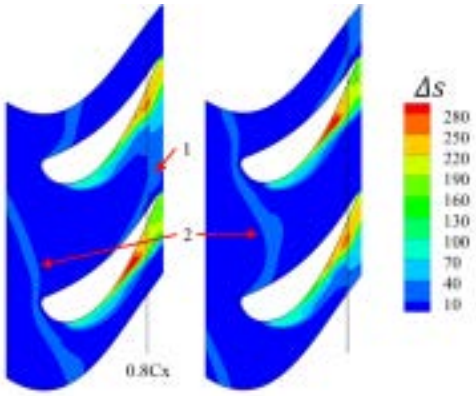

(a) t/τ_0=10/48 (b) t/τ_0=34/48

Fig. 12 Entropy (Jkg^{-1}K^{-1}) on the Cut Plane of 95% Span for Two Time Instants

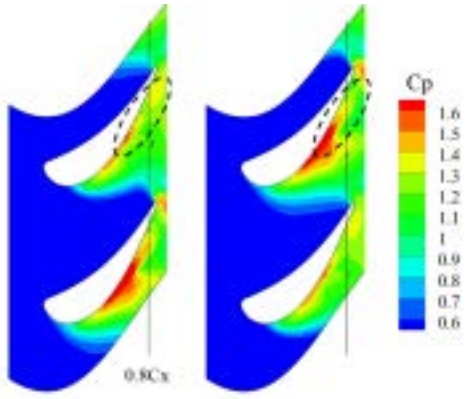

(a) t/τ_0=10/48 (b) t/τ_0=34/48

Fig. 13 Static Pressure Coefficient on the Cut Plane of 95% Span for Two Time Instants

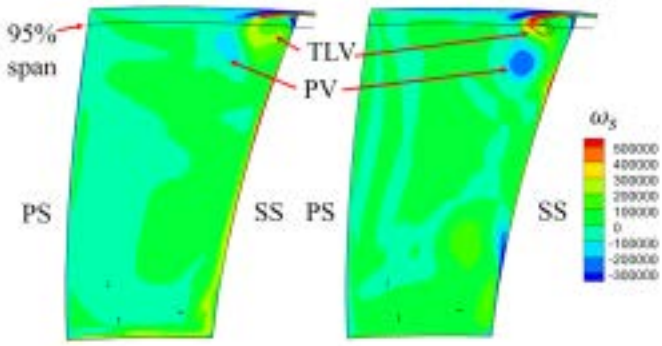

(a) t/τ_0=10/48 (b) t/τ_0=34/48

Fig. 14 Streamwise Vorticity (s^{-1}) on the Cut Plane of 0.8Cx for Two Time Instants

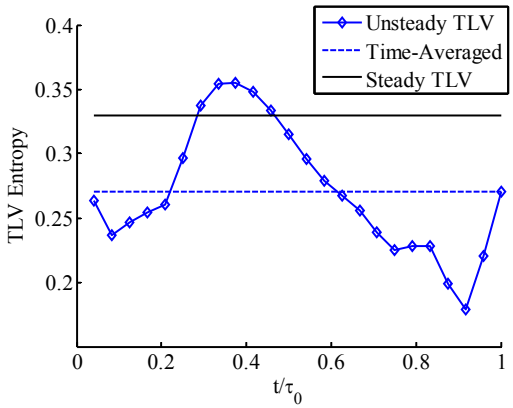

Fig. 15 Unsteady Tip Leakage Generation, Normalized by Mixed Out Entropy Generation in 'SF' Case

CONCLUSIONS

The current study investigates the unsteady effects of incoming stator vortex on the aerodynamic performance of the tip leakage in a high-pressure turbine stage. Both Reynolds-Averaged Navier-Stokes (RANS) and Unsteady Reynolds-Averaged Navier-Stokes (URANS) methods are used.

The results obtained by the steady simulations show that the tip leakage vortex and the passage vortex induce and enhance each other in the rotor passage. Tip leakage vortex breakdown occurs as the main flow diffuses, which significantly increases the loss.

The results of unsteady simulations shows that the upstream stator casing vortex suppresses the tip leakage vortex

breakdown. The incoming vortices increases the pressure within the tip leakage vortex core and reduces the streamwise adverse pressure gradient. When the stator vortex interacts with the tip leakage vortex, the tip leakage vortex breakdown is pushed further downstream and generates less entropy. On average, the tip leakage loss is reduced by 18% due to the effect of unsteady incoming vortex.

The above conclusions is obtained based on the current turbine stage design. The results clearly shown that the unsteady vortex interaction can reduce the rotor tip leakage loss. In the future, turbines with better aerodynamic performance can be design by using the mechanism of vortex interaction.

NOMENCLATURE

Cx	Rotor axial chord [m]
Cp	Static pressure coefficient [-]
Cp0	Stagnation pressure coefficient [-]
fr	Reduced frequency, $fr = f_{stator} * C_x/U_{ex,is}$ [-]
m	Mass flow rate per time[kg]
p	Static pressure [pa]
P_0	Total pressure [pa]
R	Gas constant [$Jkg^{-1}K^{-1}$]
S	Pitch [m]
t	Time [s]
T	Temperature [K]
x	Coordinate in x direction [m]

Greek Symbols

Δs	Specific entropy [$Jkg^{-1}K^{-1}$]
τ_0	Stator or bar passing period [s]
η	Entropy rise of tip leakage loss [JK^{-1}]
ω	Vorticity [s^{-1}]

Subscripts

0	Stagnation parameter
1	Inlet of domain
2	Exit of domain
in	Inlet of stator domain
s	Streamwise direction
x	Axial direction

Abbreviations

SP60	Streamwise perpendicular surface located at 60%Cx at the suction surface side
SF	Steady case with Flat tip
SNC	Steady case with No tip Clearance
TLV	Tip leakage vortex
UF	Unsteady case with Flat tip
UNC	Unsteady case with No tip Clearance

ACKNOWLEDGMENTS

The author would like to acknowledge the support of the National Science Foundation of China (NSFC), Grant No. 51576003.

REFERENCES

[1] Schaub, U. W., Vlasic, E., Moustapha, S. H., 1993, "Effect of Tip Clearance on the Performance of a Highly Loaded Turbine Stage," Technology Requirements for Small Gas Turbine, AGARD CP-537, 1993, Paper 29.

[2] Huang, A. C., Greitzer, E. M., Tan, C. S., Clemens, E. F., Gegg, S. G., and Turner, E. R., 2012, "Blade Loading Effects on Axial Turbine Tip Leakage Vortex Dynamic and Loss," Proceeding of ASME Turbo Expo 2012, June 11-15, 2012, Copenhagen, Denmark, GT2012-68302.

[3] Gao, J., Zheng, Q., Dong, P., and Zha, X., 2014, "Control of Tip Leakage Vortex Breakdown by Tip Injection in Unshrouded Turbines," Journal of Propulsion and Power, Vol. 30, November-December, pp. 1510-1519.

[4] Key, N. and Arts, T., 2006, "Comparison of Turbine Tip Leakage Flow for Flat Tip and Squealer Tip Geometries at High-Speed Conditions," Journal of Turbomachinery, Vol. 128, pp. 213-220.

[5] Schabowski, Z., and Hodson, H., 2007, "The Reduction of Over Tip Leakage Loss in Unshrouded Axial Turbines Using Winglet and Squealers," ASME Paper GT2007-27623.

[6] Camci, C., Dey, D., Kavurmacioglu, L., 2005, "Aerodynamics of Tip Leakage Flows Near Partial Squealer Rims in an Axial Flow Turbine Stage," Journal of Turbomachinery, Vol.127, 2005, pp. 14-24.

[7] Zhou, C., Hodson, H., Tibbott, I., Stokes, M., 2012, "Effects of Endwall Motion on the Aero-Thermal Performance of a Winglet Tip in a HP Turbine," Journal of Turbomachinery, Vol. 134, No. 6, 2012, pp. 061036-1-12.

[8] Zhang, M., Liu, Y., Zhang, T., Zhang, M., 2016, "Aerodynamic Optimization of a Winglet-Shroud Tip Geometry for a Linear Turbine Cascade," GT2016-5628.

[9] Denton, J. D., 1993, "Loss Mechanisms in Turbomachines," Journal of Turbomachinery, Vol. 115, Oct. 1993, pp. 621-656.

[10] Binder, A., 1985, "Turbulence Production Due to Secondary Vortex Cutting in a Turbine Rotor," Journal of Engineering for Gas Turbines & Power, Vol. 107, Oct. 1985, pp. 1039-1046.

[11] Sharma, O. P., Butler, T. L., Joslyn, H. D., Dring, R. P., 1985, "Three-Dimensional Unsteady Flow in an Axial Flow Turbine," Journal of Propulsion and Power, Vol. 1, Jan.-Feb., 1985, pp. 29-38.

[12] Dunn, M., 2001, "Convective Heat Transfer and Aerodynamics in Axial Flow Turbines," Journal of Turbomachinery, Vol. 123, Vol. 5, 2001, pp. 637-686.

[13] Hodson, H., 1984, "Boundary Layer and Loss Measurements on the Rotor of an Axial-Flow Turbine," Journal of Engineering for Gas Turbines & Power, Vol. 106, No. 2, 1984, pp. 80-80.

[14] Hodson, H., and Howell, R., 2005, "Bladerow Interactions, Transition, and High-lift Aerofoils in Low Pressure Turbines," Annual Reviews, pp. 71-98.

[15] Jenney, P., Abhari, R., Rose, M., Brettschneider, M., Engel, K., Gier, J., 2013, "Unsteady Rotor Hub Passage Vortex Behavior in the Presence of Purge Flow in an Axial Low Pressure Turbine," Journal of Turbomachinery, Vol. 135, No. 5, 2013, pp. 051022-1-9.

[16] Schlienger, J., Kalfas, A., Abhari, R., 2005, "Vortex-Wake-Blade Interaction in a Shrouded Axial Turbine," Journal of Turbomachinery, Vol. 127, No. 5, 2005, pp. 699-707.
[17] Pullan, G., Denton, J. D., 2003, "Numerical Simulations of Vortex-Turbine Blade Interaction," 5th Euro. Turbo. Conf., 2003, pp. 1049-1059.Volino, R. J., Galvin, C. D., Brownell, C. J., 2014, "Effects of Unsteady Wakes on Flow Through High Pressure Turbine Passage With and Without Tip Gaps," Proceeding of ASME Turbo Expo 2014, June 16-20, 2014, Dusseldorf, Germany, GT2014-27006.
[18] Chaluvadi,V. S. P., Kalfas, A. I., Hodson, H. P., 2003, "Blade Row Interaction in a High-Pressure Steam Turbine," Journal of Turbomachinery, Vol. 125, Jan. 2003, pp. 14-24.
[19] Chaluvadi,V. S. P., Kalfas, A. I., Hodson, H. P., 2004, "Vortex Transport and Blade Interactions in High Pressure Turbines," Journal of Turbomachinery, Vol. 126, Jul. 2004, pp. 395-405.
[20] Yoon, S., Vandeputte, T., Mistry, H., 2015, "Loss Audit of a Turbine Stage," Proceeding of ASME Turbo Expo 2015, June 15-19, 2015, Montreal, Canada, GT2015-43349.
[21] Zeschky, J., Gallus, H. E., 1991, "Effects of Stator Wakes and Spanwise Nonuniform Inlet Conditions on the Rotor Flow of an Axial Turbine Stage," International Gas Turbine and Aeroengine Congress and Exposition, June 3-6, 1991, Orlando, FL.
[22] Volino, R. J., Galvin, C. D., Brownell, C. J., 2014, "Effects of Unsteady Wakes on Flow Through High Pressure Turbine Passage With and Without Tip Gaps," Proceeding of ASME Turbo Expo 2014, June 16-20, 2014, Dusseldorf, Germany, GT2014-27006.
[23] Liu, Z, Liu, Z, Feng, Z, 2014, "Unsteady Analysis on the Effects of Tip Clearance Height on Hot Streak Migration Across Rotor Blade Tip Clearance," Journal of Engineering for Gas Turbines & Power, Vol. 126, No. 8, pp. 082605-1-11.
[24] Menter, F.R., 1994, "Two-Equation Eddy-Viscosity Turbulence Models for Engineering Applications," AIAA Journal, Vol. 32, pp. 1598–1605.
[25] Smith, C.I., Chang, D., 2012, "Effects of Non-Uniform Inlet Temperature Distribution on High-Pressure Turbine Blade Loading," International Journal of Turbo Jet-Engines, 2012; 29(3): 189-205.
[26] Zhang, Q., O'Dowd, D. O., Wheeler, A. P. S., 2011, "Overtip Shock Wave Structure and Its Impact on Turbine Blade Tip Heat Transfer," Journal of Turbomachinery, 2011, vol. 133, 041001-1-8.
[27] Zhou, K., Zhou, C., "Transport Mechanism of Hot Streaks and Wakes in a Turbine Cascade", Journal of Propulsion and Power, Vol. 32, No. 5, 2016, pp. 1045-1054.